

Article

***n*-Alkane Distribution—A Paleovegetation Change Indicator during the Period from Late Glacial to Late Holocene on Russian Plain (Bryansk Region)**

Ekaterina Stolpnikova ^{1,2,*}, **Natalia Kovaleva** ² and **Ivan Kovalev** ²

¹ A.N. Severtsov Institute of Ecology and Evolution RAS, Leninskiy Prospekt, 33, 119071 Moscow, Russia

² Faculty of Soil Science, Lomonosov Moscow State University, Leninskiye Gory, 1-12, GSP-1, 119991 Moscow, Russia; natalia_kovaleva@mail.ru (N.K.); kovalevmsu@mail.ru (I.K.)

* Correspondence: opallada@yandex.ru

Received: 16 January 2020; Accepted: 28 January 2020; Published: 26 February 2020



Abstract: Loess-paleosol series are well preserved in the south part of the Russian Plain. However, these sequences have a low number of studies on their organic matter, such as researches of isotope composition, *n*-alkane and other biomarkers. Thus, the purpose of the study was to reconstruct vegetation conditions from the Late Glacial to Late Holocene. We used the leaf wax-derived *n*-alkanes to detect vegetation evolution of the Bryansk Region. The stable carbon isotope composition of organic matter and pedogenic carbonates was carried out for the same aim. Three paleosols (of Lasko, Bølling-Allerød warmings and Holocene second humus horizons) and modern soils of different relief positions were investigated. *n*-Alkane distribution, as well as isotope composition indicates changes from grassy to woody vegetation during this period. The use of biomarkers such as *n*-alkanes helps to more clearly interpret isotopic data.

Keywords: palaeosol; *n*-alkanes; biomarkers; Late Pleistocene; loess-soil series; stable isotopes

1. Introduction

The loess-soil series are well represented on the Russian Plain, particularly in the south and south-west, and reflect the Late Pleistocene climatic restructuring by numerous climatic oscillations near Pleistocene–Holocene boundary. Many researchers [1–3] have found that Late Valdai (~23–10 kyr BP, Wurm IV, Late Glacial) loess deposits in this region are heterogeneous and separated by humic or gley horizons (undeveloped soils) in many stratigraphic sections. These horizons are markers of regional climatic fluctuations between 17–10.2 kyr BP.

Despite the abundance of paleogeographic studies of the Late Pleistocene loess-paleosol series on the Russian Plain [1,4–8], there are currently no paleoreconstructions based on *n*-alkane distribution. Although similar studies have been carried out for modern soils that were interested in anthropogenic pollution [9,10].

The final stage of Wurm (Valdai) glaciation is a period of sharply continental climate on the East European Plain in Pleistocene history [11,12]. The icecap reached the line, passing sublatitudinally from Vilnius to Smolensk, further to the north-west to the Rybinsk Reservoir and across Lake Kubenskoe to the northeast [12]. The southern edge of the permafrost zone reached Rostov and Volgograd—46°–48° N while the thickness of permafrost at the latitude of Moscow was 300 m [11].

The organic matter of the Late Pleistocene loess-paleosol series is a well-known proxy of paleoclimatic information. At the same time, the low content of Pleistocene organic matter in interstadial soils creates difficulties during such kinds of research. In this case, the content and distribution of leaf wax *n*-alkanes, the isotopic composition of organic carbon and carbonates are more useful methods for paleovegetation reconstructions [13–15].

The isotopic composition of organic carbon and different chemical parameters allowed us to reconstruct the dominance of meadow hydromorphic landscapes during the interstadials Lasko (18–16 kyr BP) and Bølling-Allerød (12.4–10.9 kyr BP), which is presented in our previous research—but this is not consistent with the trend of widespread climate aridification in the Late Pleistocene [16]. The composition of *n*-alkanes makes it possible to clarify the features of biocenoses.

Aliphatic hydrocarbons with a carbon chain length of 16 to 34 atoms, despite their low content in the organic matter (OM) of soils [17], are convenient compounds for studying of the paleovegetation. *n*-Alkanes are one of the most hydrophobic organic molecules of the soil lipid fraction which allows them to form strong complexes with solid phase of the soil and limits their migration in solutions due to their low solubility in water [13]. Being products of biogenic synthesis, *n*-alkanes have not formed in the soil during intracellular and extracellular degradation of organic compounds [13]. Thus, the distribution in the soil and seasonal changes in the homological composition of alkanes can reflect the localization and dynamics of the transformation and stabilization of organic matter from the moment it enters the soil [13]. The main sources of *n*-alkanes in soils are the overground parts of plants, the root and bacterial biomass [18–20]. Unbranched alkanes with a long C–C chain provide the hydrophobic properties of leaf waxes and serve as the primary barrier of plants from environmental conditions, protecting the leaf from moisture loss by transpiration [21]. Long chain *n*-alkanes C_{21–34} are synthesized as a part of epicuticular waxes on the leaves of terrestrial plants, and are the most distinguishable and widely used plant biomarkers entering the soil with plant residues [22,23].

On the surface of the plant cuticle, lipids such as cutin and suberin are associated with other, less polar compounds-waxes. In the leaf waxes of terrestrial plants, *n*-alkanes with a chain length of C_{25–33} have maximum concentrations. Alkanes are localized in the litter and then enter the soil, where they are considered the most degradation-resistant component [13]. Plants usually produce a set of *n*-alkanes in accordance with a strict coefficient of the predominance of odd compounds and often with the dominance of one (two) specific homologs [22]. For example, for herbaceous plants, C₃₁ predominates in the total spectrum of *n*-alkanes, for woody plants C₂₉ and C₂₇ [23]. The predominance of compounds with a shorter hydrocarbon chain (23–25) was studied in the *Sphagnum* mosses spectra [24,25]. The increase in the concentration of medium chain *n*-alkanes (C_{16–24}) is associated with microbial activity [23,26]. The synthesis of hydrocarbons in microorganisms depends on environmental conditions that determine the pathways of physiological regulation. Gram-positive bacteria, such as *Clostridium*, produce intracellular hydrocarbons with a chain length of 11–35 carbon atoms with a predominance of medium chain (C_{18–27}) or long chain compounds C_{25–35} [27,28]. The Gram-negative anaerobic bacteria sulfate-reducers—*Desulfovibrio desulfuricans*—also produce C_{11–35} hydrocarbons and more than 80% of their total content is C_{25–C₃₅} *n*-alkanes [29–31]. Various systematic groups of microorganisms are characterized by a specific composition of the hydrocarbon fraction, for example, cyanobacteria are unique producers of 7- and 8-methyl-heptadecans, photosynthetic bacteria differ in the synthesis of cyclic hydrocarbons [32], and long-chain hydrocarbons dominate in fungi [33]. It is important to note that microorganism cells are characterized by a low content of hydrocarbons (not more than 10% of dry weight) [34].

Due to the linear structure with a small number of functional groups, *n*-alkanes are especially stable and long-lived molecules that can persist in the soil for thousands of years [24,35]. In the surface horizons, the main source of n-alkanes is the litter, which determines the composition and content of hydrocarbons. Moreover, the ratio of dominant hydrocarbon chains remains [23]. The mechanisms of the entry and transformation of *n*-alkanes in the lower horizons are not clearly covered in the literature. A large role in this regard is given to earthworms and microorganisms [17,36–38]. The spectrum of n-alkanes differs from that observed in the upper horizons: the proportion of medium chain (C_{17–24}) and even compounds increases [17,22,38,39].

In the process of the decomposition of plant material by microorganisms, the total amount of hydrocarbons decreases, and the content of individual compounds with a specific chain length does not change significantly [23,40].

Aquatic plants are characterized by the lower content of long-chain alkanes (C_{27-33}) in comparison with terrestrial ones [41]. The predominance of even alkanes over odd can indicate the degradation of organic matter over time [14]. The authors of another publication [10] discuss that the predominance of even alkanes indicates the contribution of microbial biomass. In this case, the proportion of medium-chain alkanes ($< C_{25}$) also increases.

Thus, based on such strong conservation as described above, *n*-alkanes have been actively used as biomarkers of plant communities and climatic conditions in paleoreconstructions in recent decades.

Alkanes are found in modern and fossil plant materials [42,43], in soils [9,10,21,39], lacustrine sediments [44], peat sediments and peaty soils [25,40,45], marine sediments [46,47] as well as paleosols [13,41,48] and loess-paleosol series [15,49].

The purpose of this study was to reconstruct the paleovegetation changes in the loess-paleosol series of the Bryansk region (Russia) during the transition from the Lasko and Bølling-Allerød warm periods (Late Pleistocene) to the Late Holocene using the method of *n*-alkanes distribution in organic matter of modern and paleosols.

2. Materials and Methods

Two investigated loess-sandy-paleosol sequences are located on the southeast part of the East European Plain (Bryansk region, Russia) in the place called Trubchevskoe Opolye (Figure 1). Trubchevskoe Opolye is situated on the high right bank of Desna River (the watershed of the rivers Desna and Sudost) and represented by a landscape typical for Russian Plain with a paleocryogenic microrelief [8,50]. The study area is covered by a system of micro-elevations and micro-depressions (Figure 2a,b), which can reach a diameter of 5–10 m and depth up to 30 cm. An important feature of these landscapes is the presence of second humus horizons in the soils of micro-depressions at depths of 50–80 cm and the absence of such horizons at micro-elevations.

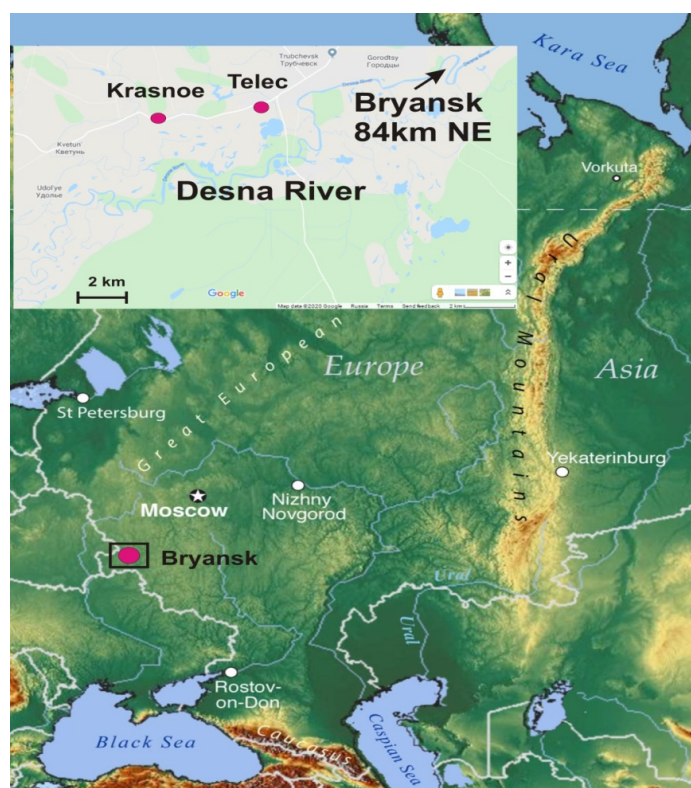


Figure 1. Location of studied sites, internet source; <https://www.nationsonline.org/oneworld/map/European-Russia-map.htm>.

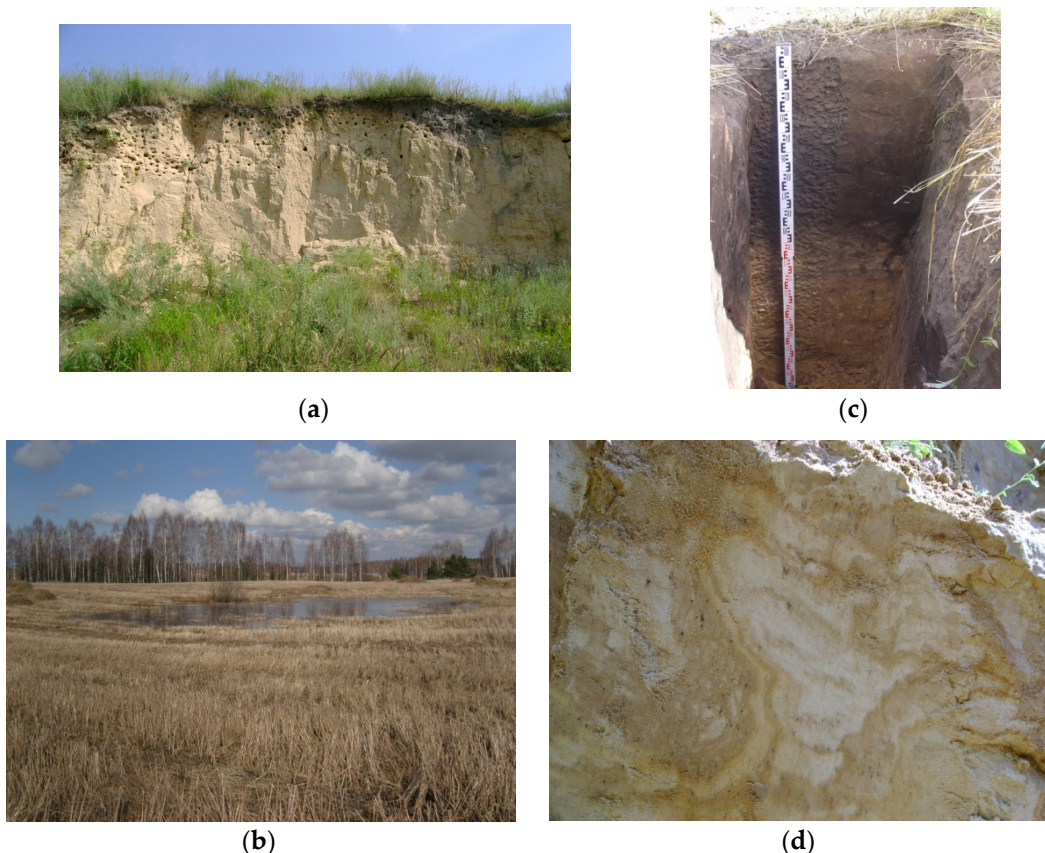


Figure 2. (a) Micro-depression in upper part of quarry; (b) micro-depression in landscape; (c) second humus horizon, micro-depression profile; (d) Cryoturbation within sandy deposits, Krasnoe outcrop.

The average annual temperature in the study area is +5.4 °C. The amount of precipitation ranges from 550 to 590 mm [50]. Native soils for this region (right bank of Desna)—are gray forest soils under broadleaf forests of the forest-steppe zone (WRB: Albic Luvisols/Grey Luvic Phaeozems), but now these soils have almost all been plowed up and are called agrogrey soils.

Also, the original feature of the investigated area is formation of different subtypes of soils associated with positions in microrelief: varieties with the second humus horizon are formed in plate-shaped micro-depressions; gleyic variants are formed in the middle parts of slopes and gley ones—at the footslopes and deeper depressions. The systems of micro-depressions and micro-elevations are well traced in the walls of the quarries Krasnoe and Telec on the right bank of the Desna River (Figure 2a). Second humus horizons were indicated in micro-depression and depression of relief at the depth range 50–85 (Ab, Location 2 in Table A1 and Figure 2c) and 40–64 cm respectively (Ab, Location 3, Table A1).

The sample points (52°33'70'' N, 33°42'62'' E and (52°34'51'' N, 33°44'71'' E) of loess-paleosol series are located near villages Krasnoe and Telec, respectively (Figure 1). The soil profiles of micro-depression and micro-elevation located above the loess-soil series of quarries were sampled at altitudes of 182 and 175 m, respectively. Additionally, a profile of unplowing soil in a deeper depression was taken (altitude 142 m, Location 3 in Table A1, Table A2—this profile is called depression).

The sand-loess deposits opened in quarries near the villages Krasnoe (first terrace of Desna) and Telec (second terrace) formed in the second and first half of the Valdai (Wurm) period, respectively [2]. Loess deposits of quarries cover the sandy sediments with numerous signs of permafrost, such as disturbance by cryoturbation processes (Figure 2d), gleaming and ferruginous horizons. Location 1 – Telec quarry stratigraphy contains modern soil of micro-elevation (0–120 cm). Modern soil has formed on loess-like sediment (120–250 cm, C1-3). The paleosol of the Lascaux interstadial is fixed at

depths of 250–300 cm (Bb-BCb) and represented by light brown sandy loam sediment with a cemented ferruginous sand horizon ORTZ1 (350–420 cm). The underlying stratum is composed of sand with traces of gleying. Location 2—Krasnoe quarry stratigraphy contains modern soil of micro-depression (0–220 cm) with dark brown Holocene paleosol or second humic horizon (Ab 50–85 cm, Figure 2c). The underlying loess-like deposits (220–470 cm, C1-2) contain iron-manganese spots along the pores, clay cutans. Cryoturbated soil of Bølling-Allerød is fixed at depths 470–495 cm (Bb) and 495–500 cm (BCb). Paleosol is represented by reddish-brown loam with ferruginous spots. The underlying sand stratum (500–570 cm) also contains waterlogging traces - bluish, reddish colors and ferruginous horizons. Location 3—is a modern soil (0–110 cm) with second humic horizon (Ab, 40–65 cm) (Table A1).

Thus, these loess-paleosol sequences reflect the transition from Late Pleistocene to Holocene warming for Desna river landscapes with warmer periods and permafrost melting episodes. Sand deposits with traces of gleying alternate with two Late Pleistocene paleosols and are covered with loess-like loam on which Holocene paleosols and modern soils are formed. The paleosol of the Krasnoe loess-soil series was found in cryoturbated sand deposits, while the Telec quarry soil divides the sand deposits from the upper loess-like sediments and has flat borders.

A radiocarbon analysis of extractable humic acids was carried out by the method of liquid scintillation counting at the Kyiv Radiocarbon Laboratory (Institute of Environment Geochemistry, Ukraine) [51]. The content of the ^{14}C isotope was measured on a Quantulys 1220 T spectrometer. Data calibration was done using OxCal v4.2.4 program [52] with IntCal13 curve [53]. Humic acids were chosen as a sample for dating due to the absence of other organic residues (such as bones, coal) which are more common for the cultural layers of archeological sites.

The qualitative and quantitative determination of *n*-alkanes was carried out by capillary gas–liquid chromatography. The extraction carried out with chloroform using an automatic extractor ASE 200 at a temperature of 100 °C. Separation of the nonpolar fraction of hydrocarbons carried out on aluminium oxide Al_2O_3 (Brokman activity level-II). The analysis was carried out on an Agilent 6890 gas chromatograph with a flame ionization detector and a column DB-1 ms (length—30 m, diameter—0.25 mm, phase thickness—0.25 μm). A standard mixture of *n*-alkanes $\text{C}_{12}\text{--C}_{36}$ was used for calibration with individual alkanes.

n-Alkanes (normal alkanes)—unbranched saturated aliphatic hydrocarbons are biomarkers of such plant groups as trees, mosses, grasses, which have a different ratio of these hydrocarbons. It is known that $n\text{C}_{27}\text{-}n\text{C}_{29}$ *n*-alkanes dominate in most modern trees and shrubs, and $n\text{C}_{31}\text{-}n\text{C}_{33}$ *n*-alkanes—in grasses [18] and are resistant to biodegradation. Data are presented in $\mu\text{g}/\text{kg}$ of dry weight.

To assess the predominant source of *n*-alkanes and the characteristics of the total spectrum and to estimate the degradation OEP index (odd-over-even predominance) is used: $\text{OEP} = (n\text{C}_{25} + n\text{C}_{27} + n\text{C}_{29} + n\text{C}_{31} + n\text{C}_{33})/(n\text{C}_{24} + n\text{C}_{26} + n\text{C}_{28} + n\text{C}_{30} + n\text{C}_{32})$ [13]. We also used informative indices such as $\text{ACL}_{27\text{-}33}$ (average chain length), $\text{CPI}_{27\text{-}33}$ (carbon preference index), and P_{aq} (contribution of aquatic plants).

To determine the carbon isotopic composition of soil carbonates samples were kept in a muffle stove at 500 °C for 1 hour to remove organic matter. The $^{13}\text{C}/^{12}\text{C}$ ($\delta^{13}\text{C}$) ratio was measured on a mass spectrometer Thermo-Finnigan Delta V Plus IRMS and an elemental analyzer Thermo Flash 1112. Standard-PDB. The carbon isotope ratio is a well known marker for searching of C3 or C4 vegetation transitions.

3. Results

As is evidenced from the Figures 3 and 4 that show distribution of magnetic susceptibility values (x), mineral phosphorus content, organic carbon isotope composition of Telec quarry sequence (Figure 3) and Krasnoe quarry sequence (Figure 4) based on previous [13–16] and new data, buried soils are well distinguished by these paleoindicators as well as by the organic carbon and phosphorus content (Appendix A, Table A1).

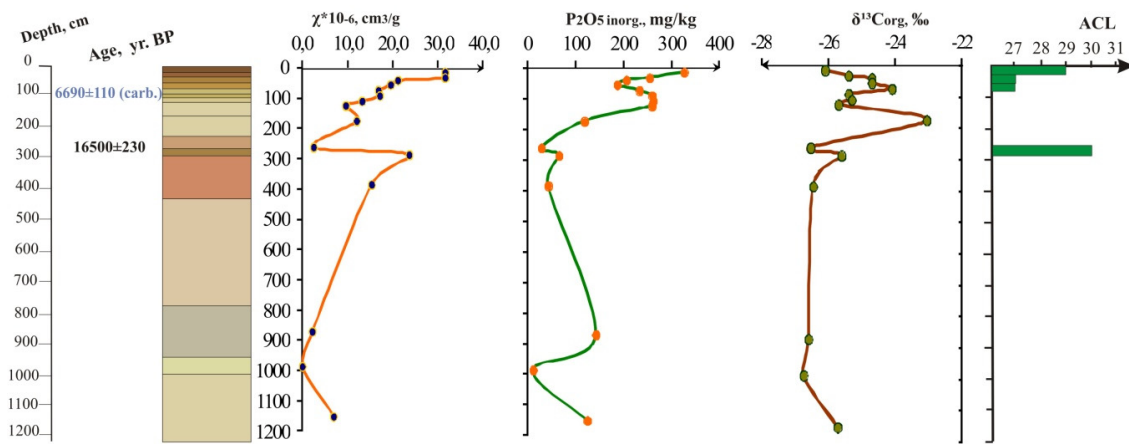


Figure 3. Loess-paleosol sequence with micro-elevation (on the top), Telec quarry, magnetic susceptibility, inorganic phosphorus, stable carbon isotope curves, average chain length in *n*-alkane distribution.

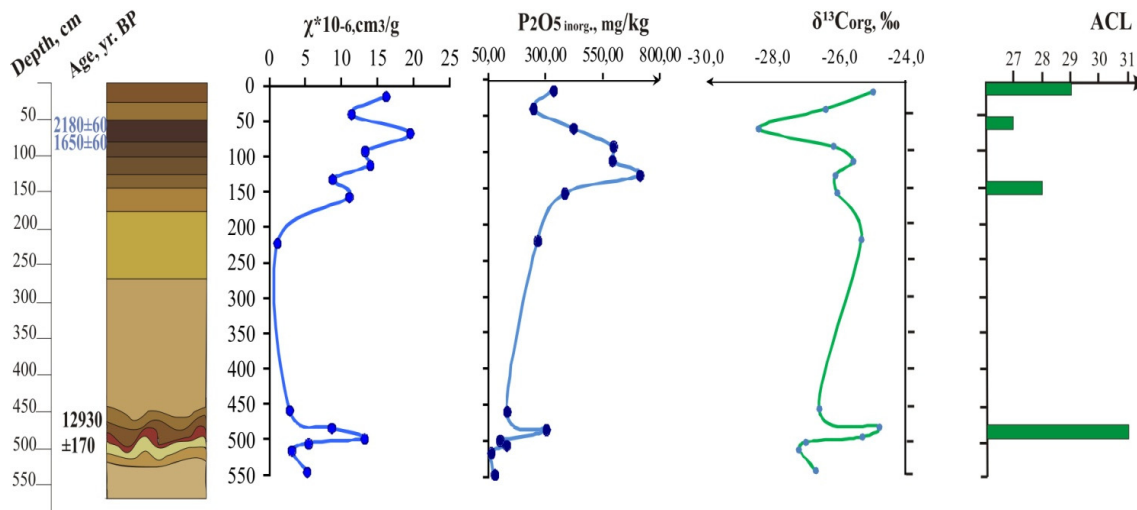


Figure 4. Loess-paleosol sequence with micro-depression (on the top), Krasnoe quarry, magnetic susceptibility, inorganic phosphorus, stable carbon isotope curves, average chain length in *n*-alkane distribution.

According to dating results, the second humus horizon of the micro-depression soil corresponds to the Holocene Subatlantic period. The soil of the micro-elevation has no second humic horizon (the common feature of the investigated landscapes), but it has a thin Atlantic horizon at a depth of 85–99 cm with age 6690 ± 110 (Table 1).

More ancient paleosol of the Last Glacial period in the Krasnoe outcrop (Figure 4) under the micro-depression profile has data 12930 ± 170 years BP and marks the Bølling–Allerød warm period. The sequence of Telec outcrop under the micro-elevation soil contains Lasko (Lascaux) interstadial soil (i.e., the Trubchevsk horizon—in Russian stratigraphic scales) $16,500 \pm 230$ BP (Table 1). These two Late Pleistocene soils correspond to MIS2 according to [54,55]).

Table 1. Radiocarbon data for paleosols of Bryansk region.

Sample	Depth (cm)	Lab. Number	Material	Radiocarbon Age (yr)	Calendar Age (yr)
Ab, micro-depression	50–85	Ki-18775	Humic acids	1650 ± 60	$1\sigma^1$ 334–530 BC 2σ 257–539 BC
Ab, micro-depression	50–85	Ki-17415	Humic acids	2180 ± 60	1σ 360–270 BC 2σ 390–90 BC
Ab, micro-elevation	85–99	Ki-18776	Carbonates	6690 ± 110	1σ 5706–5527 BC 2σ 5837–5392 BC
Bb2, Krasnoe	470–495	Ki-17413	Humic acids	12930 ± 170	1σ 14000–13200 BC 2σ 14200–12400 BC
Bb, Telec	250–275	Ki-17414	Humic acids	16500 ± 230	1σ 18150–17300 BC 2σ 18600–16900 BC

¹ 1σ —probability 68.2%; 2σ —probability 95.4%.

n-Alkanes measurement was carried out in the range of chain length 17–34. The maximum concentration of *n*-alkanes was recorded for the Holocene paleosol—the second humus horizon of modern soil in depression (2668.6 µg/kg or 2.67 µg/g dry weight) (Table A2). An analysis of *n*-alkanes distribution allows us to conclude that the organic matter of the second humus horizon in the depression is better preserved than in the plowed upper part of the profile of micro-depression. We also fixed the strong predominance of mid-chain *n*-alkanes in horizons under modern humic horizon (AE, EB) (Figures 5 and 6). Therefore, we will further use data on the second humus horizon from the depression profile (Ab, 40–65 cm, Figure 7), where this horizon has a predominance of C₂₇ and C₂₉ alkanes.

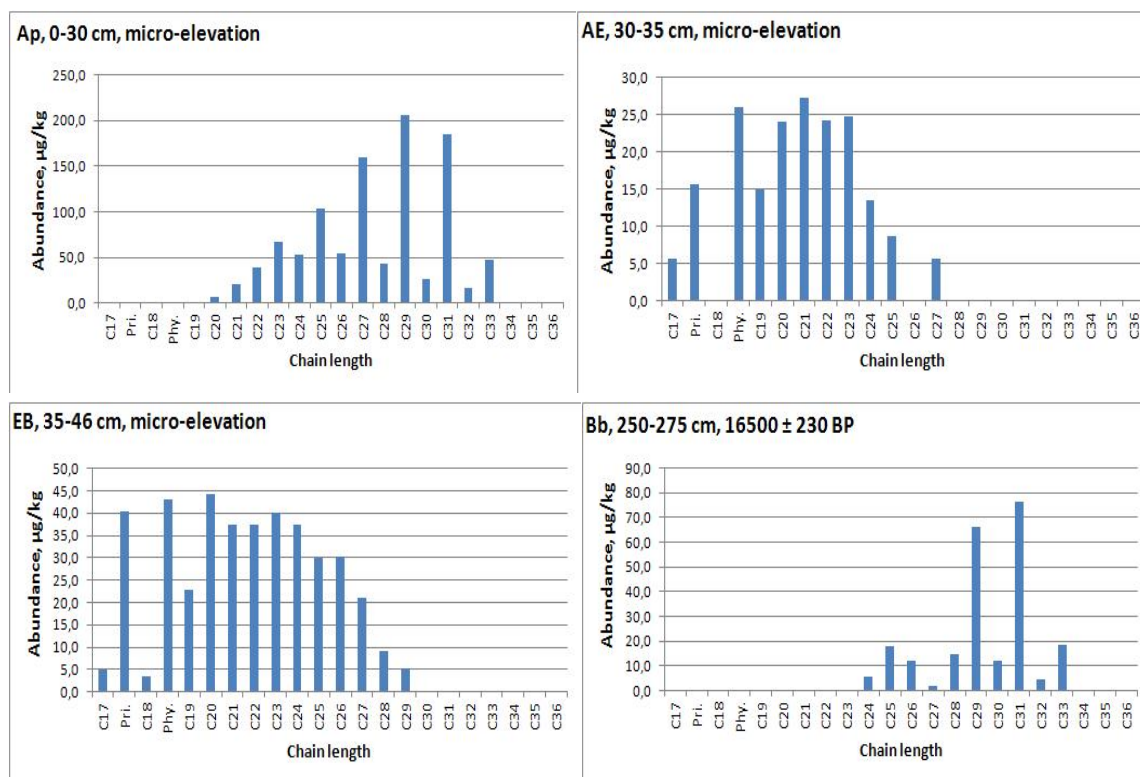


Figure 5. *n*-alkane distribution in soil of micro-elevation and interstadial soil from loess-paleosol sequence under it.

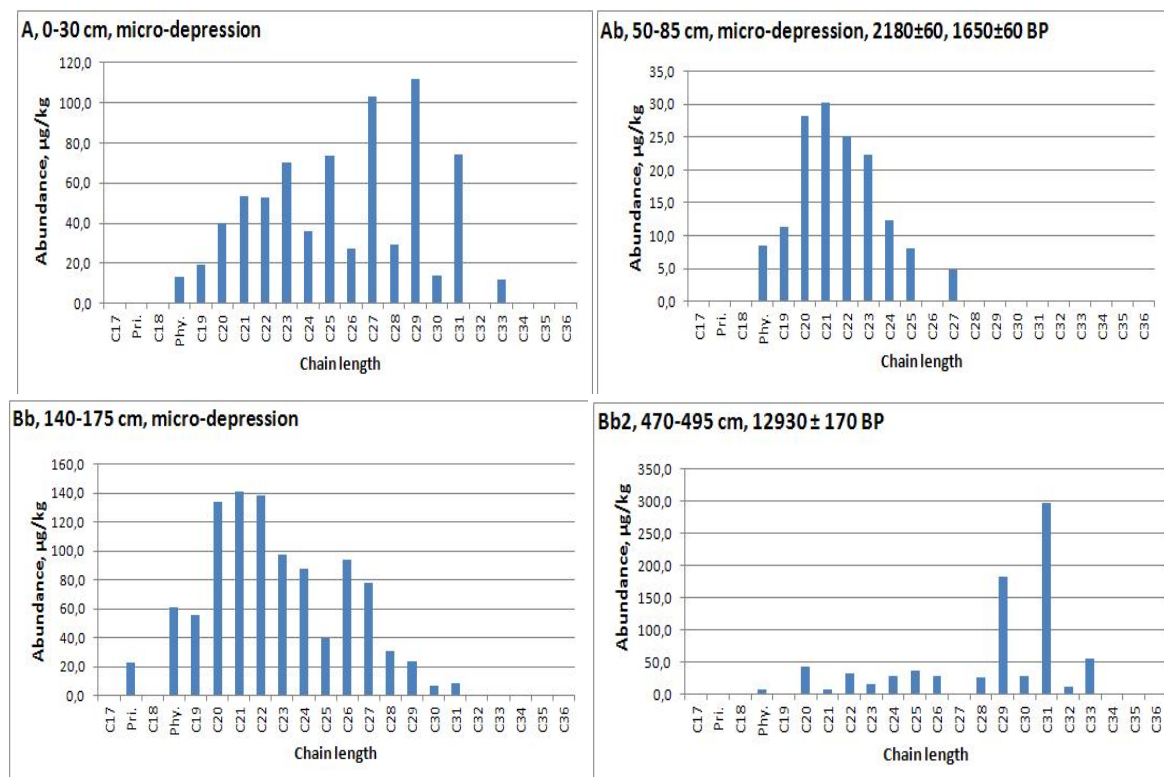


Figure 6. *n*-Alkane distribution in soil with second humus horizon (Ab) of micro-depression and interstadial soil from loess-paleosol sequence under it.

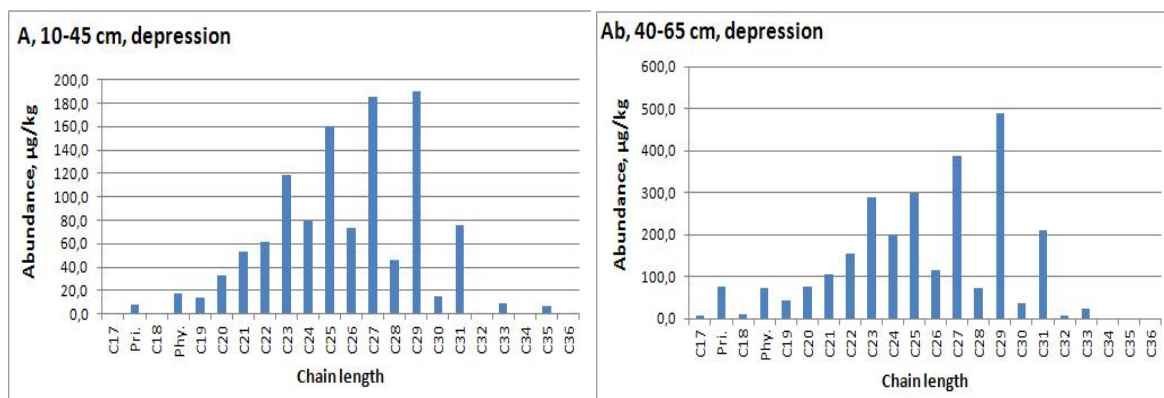


Figure 7. *n*-Alkane distribution in native soil with second humus horizon (Ab), depression.

The maximum concentration of alkane C₃₁ (coming mainly from grassy vegetation) was measured for the Late Pleistocene interstadial paleosols of the Krasnoe and Telec quarries (Table A2). The index C₃₁/C₂₉ for these soils are 1.64 and 1.15, respectively, while in the Holocene samples it is less than 1. Paleosols are characterized by a predominance of odd alkanes which indicates the origin from vascular plants (OEP = 4–6).

Average chain length (ACL) shows the transition from 31 and 30 for the Late Pleistocene soils to 29, 27—for the Holocene soils. Furthermore, the maximum value of index $(nC_{31} + nC_{33}) / (nC_{27} + nC_{29})$ was fixed for Late Pleistocene soils. We also calculated an index which characterized the contribution of aquatic plants (Pq) [44]. It was a fixed, low contribution of these plants in the Late Pleistocene, and slightly larger influence in the Holocene soils—with the exception of AE horizons with possibly degraded organic matter and high mid-chain alkane concentrations (Table A2, Figure 5).

The loess covered Lasko interstadial soil has a maximum value of $\delta^{13}\text{C}_{\text{carb}}$. ($-8.3\text{\textperthousand}$) as well as heaviest organic carbon isotope composition ($-23.1\text{\textperthousand}$) reflected most arid episode after Lasko warming (Table A1). However, the paleosol of the Lasko warm period has a very light weight isotope composition of pedogenic carbonates. Such isotope values require further investigation, However, few similar data are known on pedogenic carbonates recorded in sediments and paleosols of the Late Pleistocene-Early Holocene [56,57].

4. Discussion

By analyzing current and previously obtained data, we can conclude that the Bølling-Allerød warm period was characterized by a drier and warmer climate than the Lasko interstadial (i.e., the Trubchevsk interstadial—regional name). Despite the cryogenic disturbance, the paleosol of Bølling-Allerød has the features of soil formed in more favorable and warm conditions: higher values of organic phosphorous (106 mg/kg, Table A1), magnetic susceptibility (Figure 4), total amount of *n*-alkanes. Stable carbon isotopic composition reflects ($\delta^{13}\text{C}_{\text{org}} = -24.8\text{\textperthousand}$; $\delta^{13}\text{C}_{\text{carb.}} = -8.8\text{\textperthousand}$) an increase of arid conditions in comparison with the overlying and underlying deposits and Lasko paleosol (Table A1). Furthermore, it has the largest proportion biomarkers ($(n\text{C}_{31} + n\text{C}_{33}) / (n\text{C}_{27} + n\text{C}_{29}) = 1.95$, ACL = 31) in comparison to other recorded paleosols (Table A2) which indicates the dominance of herbaceous plant communities. Thus, the landscapes were productive and allowed for soil formation. The well-spatially-expressed and undisturbed soil of the Lasko interstadial had apparently crowned the permafrost level; therefore, it has flat boundaries. Its formation took place in a more hydromorphic environment and was accompanied by processes of carbonates and iron accumulation influenced abnormally light carbonate isotope composition (Table A1). Nevertheless, the C₃₁/C₂₉ index in Lasko soil (1.15) is near 1 and shows the very slight predominance of grassy vegetation biomarkers. On the other hand, some authors have documented the accumulation of alkane C₂₉ in sedges [40].

Further early palynological investigations of the Russian Plain [1] correlate with our conclusion about the warmer and drier period of Bølling-Allerød in comparison with Lasko interstadial. In the Middle Dnestr valley (Ukraine), the author detected three interstadial warmings—Lasko, Bølling, Allerød, and registered the transition of vegetation from mixed forests of pine, oak, hornbeam, ash, linden, elm, etc., through to the domination of forbs-serial meadows in Bølling to complex vegetation with broad-leaved forests along river valleys and ravines in Allerød. For the Lasko period in the middle Desna valley, the author also highlights the predominance of woody vegetation (pine, cedar-pine, birch-pine forests with undergrowth from birch, alder, juniper, willow) and indicates the periglacial nature of the landscape (ephedra, *Artemisia*) [1]. Our research also suggests the coexistence of woody and herbaceous vegetation during these interstadials, which is reflected in a noticeable proportion of C₂₉ alkane ($n\text{C}_{31}/n\text{C}_{29} = 1.64$ —for Bølling-Allerød and 1.15—for Lasko soil) and not heavy values of the carbon isotope ratio (from $-26\text{\textperthousand}$ to $-24\text{\textperthousand}$) indicated the predominance of vegetation with C3-type of photosynthesis. However, at the same time, the predominance of grasslands was reflected. Based on the distribution of *n*-alkanes and the index ACL, the Bølling-Allerød soil was formed under conditions of a larger proportion of grasses compared with the soil of the Lasko interstadial and modern soils.

Based on the available palynology data [58,59], periglacial vegetation was characteristic of both studied Late Pleistocene periods in Eastern Europe and in particular the Russian Plain. The period of the last transition of the glacier (LGT, 17–12.4 kyr BP) is characterized by the predominance of tundra and forest-tundra species to the north of 48° – 49° N, sometimes passing south to the latitudes of Bryansk (52° N) along the valleys of large rivers. Steppe and meadow-steppe species prevailed south of 47° – 51° N. Thus, the studied territories are located in the boundary position between the tundra/forest-tundra and the steppe zones, and the authors [58] relate it to the periglacial forest-steppe zone. At the same time, the vegetation of the Lasko interstadial was not investigated. According to palynological data [59], the Bølling-Allerød period was characterized by a wetter and warmer climate. Nevertheless, despite a slight shift in natural zonality revealed by palynologists [59], during this warm period, the vegetation of the studied Bryansk region is referred to the periglacial forest-steppe

zone, as well as at earlier stages of Late Glacial.. Pine-birch forests dominated in combination with meadow steppes and tundra associations. Thus, the proportion of open grassy landscapes can be determined using isotopic ratios and analyses of the distribution of *n*-alkanes, which allow us to clarify the differences between objects with similar palynological characteristics.

The clearly visible dominance of woody biomarkers in Holocene soils—including modern humic horizons ((nC31 + nC33)/(nC27 + nC29) = 0.23–0.63, ACL=27–29, Table A2)—correlate with a light isotopic composition (Table A1, Figures 5–7). A similar distribution of *n*-alkanes is characteristic of woody biocenoses, which mainly carry out the C3 type of photosynthesis. The Subatlantic paleosol of the second humus horizons is characterized by a more humid and warm climate compared with the modern climate (this paleosol distinguished by a high amount of organic carbon and phosphorus, Table A1, Location 2).

The results of *n*-alkanes composition are more reliably a record of change in vegetation at the Late Pleistocene-Holocene transition, confirming the hypothesis of the dominance of biocenoses with a higher proportion of grassy landscapes. The predominance of mid-chain alkanes in AE, EB horizons of modern arable soils is probably a result of degradation associated with microbiological activity [10].

The data presented in this article do not yet characterize the numerous climatic oscillations in the transition from the Late Glacial to the Holocene, and were carried out as the first study in this direction of biomarkers investigations for the Russian Plain in order to catch changes in vegetation. Thus, our research will continue to clarify the data in the future.

Author Contributions: Conceptualization, N.K., E.S.; methodology, N.K.; investigation, E.S., N.K., I.K.; writing—original draft preparation, E.S.; N.K.; writing—review and editing, E.S., N.K., I.K.; supervision, N.K.; project administration, N.K., I.K., E.S.; funding acquisition, N.K. All authors have read and agreed to the published version of the manuscript.

Funding: This research was funded by grant number 17-14-01120 of Russian Science Foundation.

Acknowledgments: The authors are thankful to Demin V.V., Streletskiy R.A. for the help in *n*-alkanes measurements.

Conflicts of Interest: The authors declare no conflict of interest. The funders had no role in the design of the study; in the collection, analyses, or interpretation of data; in the writing of the manuscript, or in the decision to publish the results”.

Appendix A

Table A1. Characteristics of organic matter *.

Location	Age, Years BP	Horizon, Depth, cm	C _{org.} , % *	P ₂ O ₅ org, mg/kg *	δ ¹³ C _{org.} , ‰ *	δ ¹³ C _{carb.} , ‰ *	n-alkane, tot., µg/g d.w. **
1. Quarry v. Telec, micro-elevation	6690 ± 110	Ap, 0–30	1.2	115.0	-26.1	non-carb.	1.03
		AE, 30–35	0.4	17.8	-25.4	non-carb.	0.19
		EB, 35–46	0.2	18.4	-24.7	non-carb.	0.41
		BC, 46–65	0.2	10.6	-24.7	non-carb.	-
		C, 65–85	0.2	0.0	-24.1	non-carb.	-
	16,500 ± 230	Ab, 85–99	0.4	97.2	-25.4	-13.5	-
		C1, 99–120	0.3	83.9	-25.3	-10.0	-
		C2, 120–..	0.2	38.9	-25.7	-8.3	-
		C3, 100–250	0.5	29.9	-23.1	non-carb.	
		Bb, 250–275	0.3	0.0	-26.5	-22.3	0.00
		BCb, 275–300	0.4	68.0	-25.6	-22.4	0.23
		ORTZ1, 350–420	0.3	44.5	-26.5	-22.0	-
		Eg, 770–970	0.1	0.0	-26.6	non-carb.	-
		C4, 970–1000	0.1	0.0	-26.7	non-carb.	-
		C5, 1000–1300	0.2	0.0	-25.7	non-carb.	-

Table A1. Cont.

Location	Age, Years BP	Horizon, Depth, cm	C _{org.} , % *	P ₂ O ₅ org, mg/kg *	δ ¹³ C _{org.} , ‰ *	δ ¹³ C _{carb.} , ‰ *	n-alkane, tot., µg/g d.w. **
2. Quarry, v.Krasnoe, micro-depression	Ap, 0–30	1.8	178.7	−25.0	non-carb.	0.73	
		AE, 30–50	1.5	311.9	−26.4	non-carb.	0.10
	2180 ± 60, 1650 ± 60	*** Ab, 50–85	2.3	635.8	−28.4	non-carb.	0.15
	AEb, 85–100	1.3	389.8	−26.2	non-carb.	-	
		Eb, 100–125	0.4	125.4	−25.6	non-carb.	-
	EBb, 124–140	0.6	0.0	−26.1	non-carb.	-	
		Bb, 140–175	0.3	0.0	−26.1	non-carb.	1.02
	C1, 175–270	0.2	0.0	−25.3	non-carb.	-	
		C2,fe,1, 445–470	0.2	0.0	−26.6	non-carb.	-
	12,930 ± 170	Bb2, 470–495	0.4	106.3	−24.8	−8.8	0.80
3. Modern soil, depression *	BCfe,b2, 495–500	0.1	0.0	−25.3	non-carb.	-	
		Eg, 500–510	0.1	0.0	−27.0	non-carb.	-
	BCfe,b3 510–520	0.1	7.8	−27.2	non-carb.	-	
		C3 520–570	0.1	2.6	−26.7	non-carb.	-
	A, 10–45	3.4	271.2	−32.7	non-carb.	1.14	
		*** Ab, 40–65	4.0	170.0	−29.5	non-carb.	2.67
	AEg, 60–80	0.8	50.8	−27.5	non-carb.	2.15	
		Eg, 80–110	0.3	0.0	−27.0	non-carb.	-

* published data [13], ** unpublished data, *** second humic horizons of modern soils.

Table A2. n-Alkane parameters *.

Sample, Depth, cm	Relief Position	Age, Years cal. BP	n-alkane tot.(C ₁₇ –36), µg/kg d.w.	C _{max}	OEP ¹	ACL _{27–33}	CPI _{27–33}	(nC ₃₁ + nC ₃₃)/(nC ₂₇ + nC ₂₉)	P _{aq}
1. Quarry Telec									
Ap, 0–30 AE, 30–35 EB, 35–46 BCb, 275–300	micro-elevation	16,500 ± 230	1027.9	C ₂₉	4.3	29	3.5	0.63	0.30
			190.2	C ₂₁	-	27	-	0	1.0
			406.2	C ₂₀	0.7	27	1.4	0	0.93
			230.5	C ₃₁	3.8	30	2.6	1.39	0.11
2. Quarry Krasnoe									
Ap, 0–30 AE, 30–50 Ab, 50–85 Bb, 140–175 Bb2, 470–495	micro-depression	2180 ± 60, 1650 ± 60	730.0	C ₂₉	4.3	29	3.5	0.40	0.44
			97.6	C ₂₂	-	-	-	0	1.00
			151.3	C ₂₁	-	27	-	0	1.00
			1020.3	C ₂₁	0.8	28	1.4	0.08	0.81
A, 10–45 Ab, 40–65 AEg, 60–80	depression	12,930 ± 170	804.3	C ₃₁	5.7	31	4.0	1.95	0.10
			1142.6	C ₂₉	3.4	29	3.7	0.23	0.51
			2668.6	C ₂₉	4.8	29	4.8	0.27	0.46
			2153.9	C ₂₅	0.9	28	1.0	0.14	0.71
3. Modern soil, depression									

¹ OEP = (nC₂₇ + nC₂₉ + nC₃₁ + nC₃₃)/(nC₂₆ + nC₂₈ + nC₃₀ + nC₃₂); CPI_{27–33} = 0.5*(nC₂₇ + nC₂₉ + nC₃₁ + nC₃₃)/(nC₂₈ + nC₃₀ + nC₃₂ + nC₃₄); ACL_{27–33} = (27nC₂₇ + 29nC₂₉ + 31nC₃₁ + 33nC₃₃)/(nC₂₇ + nC₂₉ + nC₃₁ + nC₃₃); P_{aq} = (nC₂₃ + nC₂₅)/(nC₂₃ + nC₂₅ + nC₂₉ + nC₃₁). *—unpublished data

References

1. Bolikhovskaya, N.S. *Evolution of the Loess-Soil Formation of Northern Eurasia*; MSU Press: Moscow, Russia, 1995.

2. Velichko, A.A.; Morozova, T.D.; Nechaev, V.P.; Porozhnyakova, O.M. *Paleocryogenesis, Soil Cover and Agriculture*; Nauka: Moscow, Russia, 1996.
3. Kovaleva, N.O.; Stolpnikova, E.M.; Kovalev, I.V. Paleoecological reconstruction for the Podesenie region on the Late Pleistocene-Holocene boundary (according to carbon isotopic composition of the soil). *Povolzhskiy J. Eco.* **2013**, *4*, 402–413.
4. Morozova, T.D. *Development of the Soil Cover of Europe in the Late Pleistocene*; Nauka: Moscow, Russia, 1981.
5. Gugalinskaya, L.A. *Soil Formation and Cryogenesis in the Center of the East European Plain in late Pleistocene*; ONTI NTsBI AN SSSR: Pushchino, Russia, 1982.
6. Makeev, A.O. Pedogenic alteration of aeolian sediments in the upper loess mantles of the Russian Plain. *Quat. Int.* **2009**, *209*, 79–94. [[CrossRef](#)]
7. Sedov, S.N.; Khokhlova, O.S.; Sinitsyn, A.A.; Korkka, M.A.; Rusakov, A.V.; Ortega, B.; Solleiro, E.; Rozanova, M.S.; Kuznetsova, A.M.; Kazdym, A.A. Late Pleistocene paleosol sequences as an instrument for the local paleographic reconstruction of the Kostenki 14 key section (Voronezh oblast) as an example. *Eurasian Soil Sci.* **2010**, *43*, 876–892. [[CrossRef](#)]
8. Sycheva, S.; Khokhlova, O.; Pushkina, P.; Ukrainsky, P. Interrelations of the Bryansk paleosol (end of MIS 3) with the Holocene surface soils in micro-depressions of the central forest-steppe within the Russian Upland. *Catena* **2019**, *172*, 619–623. [[CrossRef](#)]
9. Gennadiev, A.N.; Zavgorodnyaya, Y.A.; Pikovskii, Y.I.; Smirnova, M.A. Alkanes as components of soil hydrocarbon status: Behavior and indication significance. *Eurasian Soil Sci.* **2018**, *51*, 32–41. [[CrossRef](#)]
10. Anokhina, N.A.; Demin, V.V.; Zavgorodnyaya, Y.A. Compositions of n-alkanes and n-methyl ketones in soils of the forest-park zone of Moscow. *Eurasian Soil Sci.* **2018**, *51*, 637–646. [[CrossRef](#)]
11. Velichko, A.A. *Natural Process in the Pleistocene*; Nauka: Moscow, Russia, 1973.
12. Alifanov, V.M.; Gugalinskaya, L.A.; Ovchinnikov, A.Y. *Paleocriogenesis and a Variety of Soils on the Center of East European Plain*; GEOS: Moscow, Russia, 2010.
13. Zech, M.; Rass, S.; Buggle, B.; Loscher, M.; Zoller, L. Reconstruction of the Late Quaternary paleoenvironments of Nussloch loess paleosol sequence, Germany, using n-alkane biomarkers. *Quat. Res.* **2012**, *78*, 226–235. [[CrossRef](#)]
14. Zech, M.; Buggle, B.; Leiber, K.; Marcovic, S.; Glaser, B.; Hambach, U.; Huwe, B.; Stevens, T.; Sumegi, P.; Wiesenberg, G.; et al. Reconstructing Quaternary vegetation in the Carpathian Basin, SE Europe, using n-alkane biomarkers as molecular fossils: Problems and possible solutions, potential and limitations. *E&G Quat. Sci. J.* **2009**, *58*, 148–155.
15. Zech, R.; Zech, M.; Marković, S.; Hambach, U.; Huang, Y. Humid glacials, arid interglacials? Critical thoughts on pedogenesis and paleoclimate based on multi-proxy analyses of the loess-paleosol sequence Crvenka, Northern Serbia. *Palaeogeogr. Palaeoclimatol. Palaeoecol.* **2013**, *387*, 165–175. [[CrossRef](#)]
16. Stolpnikova, E.M.; Kovaleva, N.O.; Kovalev, I.V. The Carbon Isotope Composition of Organic Matter and the Age od Paleosols from Wurm Glaciation Interstadials to Holocene (Bryansk region, Russia). *IOP Conf. Series EES* **2018**, *107*, 1–6. [[CrossRef](#)]
17. Kogel-Knaber, I. The macromolecular organic composition of plant and microbial residues as inputs to soil organic matter. *Soil Biol. Biochem.* **2002**, *34*, 139–162. [[CrossRef](#)]
18. Avato, P.; Bianchi, G.; Mariani, G. Epicuticular waxes of Sorghum and some compositional changes with plant age. *Phytochemistry* **1984**, *23*, 2843–2846. [[CrossRef](#)]
19. Bull, I.D.; van Bergen, P.F.; Nott, C.J.; Poulton, P.R.; Evershed, R.P. Organic geochemical studies of soils from the Rothamsted classical experiments. The fate of lipids in different long-term experiments. *Org. Geochem.* **2000**, *31*, 389–408. [[CrossRef](#)]
20. Jetter, R.; Kunst, L.; Samuels, A.L. *Composition of plant cuticular waxes/Biology of plant cuticle*; Wiley-Blackwell: Hoboken, NJ, USA, 2006; Volume 23, pp. 145–181.
21. Luo, P.; Peng, P.; Lu, H.Y.; Zheng, Z.; Wang, X. Latitudinal variations of CPI values of long-chain n-alkanes in surface soil: Evidence for CPI as a proxy of aridity. *Sci. China, Earth Sci.* **2012**, *55*, 1134–1146. [[CrossRef](#)]
22. Bush, R.T.; McInerney, F.A. Leaf wax n-alkane distributions in and across modern plants: Implications to paleoecology and chemotaxonomy. *Geochim. Cosmochim. Acta* **2013**, *117*, 161–179. [[CrossRef](#)]
23. Zech, M.; Pedentchouk, N.; Markovic, S.B.; Glaser, B. Effect of leaf litter degradation and seasonality on D/H isotope ratios of n-alkane biomarkers. *Geochim. Cosmochim. Acta* **2011**, *75*, 4917–4928. [[CrossRef](#)]

24. Peters, K.E.; Walter, C.C.; Moldowan, J.M. The n-alkane concentrations in buds and leaves of browsed broad leaf trees. *J. Agric. Sci.* **2000**, *135*, 311–320. [[CrossRef](#)]
25. Loez-Dias, V.; Blanco, C.D.; Bechtel, A. Different source of n-alkanes and n-alkan-2 ones in a 6000 cal. yr. BP Sphagnum-rich temperate peat bog. *Org. Geochem.* **2013**, *57*, 7–10.
26. Van Beilen, J.B.; Neuenschwander, M.; Smits, T.H.M.; Roth, C.; Balada, S.B.; Witholt, B. Rubredoxins involved in alkane oxidation. *J. Bacteriol.* **2003**, *184*, 427–440. [[CrossRef](#)]
27. Walker, J.D.; Cooney, J.J. Aliphatic hydrocarbons of *Cladosporium resinae* cultured on glucose, glutamic acid, and hydrocarbons. *Appl. Microbiol.* **1973**, *26*, 705–708. [[CrossRef](#)]
28. Bagaeva, T.V.; Zinurova, E.E. Comparative characterization of extracellular and intracellular hydrocarbons of *Clostridium pasteurianum*. *Biochemistry (Moscow)* **2004**, *69*, 427–428. [[CrossRef](#)] [[PubMed](#)]
29. Bagaeva, T.V.; Zolotukhina, L.M. The formation of hydrocarbons by sulfate reducing bacteria grown under chemolithoheterotrophic conditions. *Microbiology (Moscow)* **1994**, *63*, 993–995.
30. Bagaeva, T.V. The ability of sulfate-reducing bacteria of various taxonomic groups to synthesize extracellular hydrocarbons. *Microbiology (Moscow)* **1997**, *66*, 796–799.
31. Bagaeva, T.V. Effect of the composition of the gaseous phase on the formation of hydrocarbons in *Desulfovibrio desulfuricans*. *Appl. Biochem. Microbiol. (Moscow)* **2000**, *36*, 195–198.
32. Koser, J.; Volkman, J.K.; Rullkötter, J.; Scholzbottcher, B.M.; Rethmeier, J.; Fischer, U. Monomethyl-branched, dimethyl-branched, and trimethyl-branched alkanes in cultures of the filamentous cyanobacterium *Calothrix scopulorum*. *Org. Geochem.* **1999**, *30*, 1367–1379. [[CrossRef](#)]
33. Fisher, D.J.; Holloway, P.J.; Richmond, D.V. Fatty acid and hydrocarbon constituents of the surface and wall lipids of some fungal pores. *Microbiology* **1972**, *72*, 71–78.
34. Joes, J.G. Studies on lipids of soil microorganisms with particular reference to hydrocarbons. *Microbiology* **1969**, *59*, 145–152.
35. Eglington, G.; Logan, G.A. Molecular preservation. *Philos. Trans. Roy. Soc. London* **1991**, *333*, 315–328.
36. Wentzel, A.; Ellingsen, T.E.; Kotlar, H.K.; Zotchev, S.B.; Throne-Holst, M. Bacterial metabolism of long-chain n-alkanes. *Appl. Microbiol. Biotechnol.* **2007**, *76*, 1209–1221. [[CrossRef](#)]
37. Handley, L.; Pearson, P.N.; McMillan, I.K.; Pancost, R.D. Large terrestrial and marine carbon and hydrocarbon isotope excursions in a new Paleocene/Eocene boundary section from Tanzania. *Earth Planet. Sci. Lett.* **2008**, *275*, 17–25. [[CrossRef](#)]
38. Singh, S.N. *Microbial Degradation of Xenobiotics*; Springer: Berlin/Heidelberg, Germany, 2012.
39. Quenea, K.; Derenne, S.; Largeau, C.; Rumpel, C.; Mariotti, A. Variation in lipid relative abundance and composition among different particle size fractions of a forest soil. *Org. Geochem.* **2004**, *35*, 1355–1370. [[CrossRef](#)]
40. Jansen, B.; Hausmann, N.S.; Tonneijck, F.H.; Verstraten, J.M.; de Vooght, P. Characteristic straight-chain lipid ratios as a quick method to assess past forest—paramo transitions in the Ecuadorian Andes. *Palaeogeogr. Palaeoclimatol. Palaeoecol.* **2008**, *262*, 129–139. [[CrossRef](#)]
41. Duchko, M.A.; Gulaya, E.V.; Serebrenikova, O.V.; Strelnikova, E.B.; Preis, Y.I. Distribution of n-alkanes, steroids and triterpenoids in peat and plants of swamp “Tyomnoe”. *Proc. Tomsk Polytech. Univ.* **2013**, *323*, 40–44.
42. Huang, J.; Lockheart, M.J.; Collister, J.W.; Eglington, G. Molecular and isotopic biogeochemistry of the Miocene Clarkia Formation: Hydrocarbons and alcohols. *Org. Geochem.* **1995**, *23*, 785–801. [[CrossRef](#)]
43. Otto, A.; Simoneit, B.R.T.; Rember, W.C. Conifer and angiosperm biomarkers in clay sediments and fossil plants from the Miocene Clarkia Formation, Idaho, USA. *Org. Geochem.* **2005**, *36*, 907–922. [[CrossRef](#)]
44. Aichner, B.; Ott, F.; Slowinski, M.; Noryskievicz, A.M.; Brauer, A.; Sashce, D. Leaf wax n-alkane distributions record ecological changes during Younger Dryas at Trzechowskie paleolake (northern Poland) without temporal delay. *Clim. Past* **2018**, *14*, 1607–1624. [[CrossRef](#)]
45. Li, G.; Li, L.; Tarozo, R.; Longo, W.M.; Wang, K.J.; Dong, H.; Huang, Y. Microbial production of long-chain n-alkanes: Implication for interpreting sedimentary leaf wax signals. *Org. Geochem.* **2018**, *115*, 24–31. [[CrossRef](#)]
46. McKirdy, D.M.; Thorpe, C.S.; Haynes, D.E.; Grice, K.; Krull, E.S.; Halverson, G.P.; Webster, L.J. The biogeochemical evolution of the Coorong during the mid- to late Holocene: An elemental, isotopic and biomarker perspective. *Org. Geochem.* **2010**, *41*, 96–110. [[CrossRef](#)]

47. Vogts, A.; Badewien, T.; Rullkötter, J.; Schefuß, E. Near-constant apparent hydrogen isotope fractionation between leaf wax n-alkanes and precipitation in tropical regions: Evidence from a marine sediment transect off SW Africa. *Org. Geochem.* **2016**, *96*, 18–27. [[CrossRef](#)]
48. Blödtner, M.; Zech, R.; Kühn, P.; Schneider, B.; Zielhofer, C.; von Suchodoletz, H. The potential of leaf wax biomarkers from fluvial soil-sediment sequences for paleovegetation reconstructions—Upper Alazani River, central southern Greater Caucasus (Georgia). *Quat. Sci. Rev.* **2018**, *196*, 62–79. [[CrossRef](#)]
49. Obreht, I.; Zeeden, C.; Hambach, U.; Veres, D.; Marković, S.B.; Lehmkühl, F. A critical revaluation of paleoclimate proxy records from loess in the Carpathian Basin. *Earth-Sci. Rev.* **2019**, *190*, 498–520. [[CrossRef](#)]
50. Tyurukanov, A.N.; Bystritskaya, T.L. *Opolya of Central Russia and Soils*; Nauka: Moscow, Russia, 1971.
51. Skripkin, V.; Kovalyukh, N. Recent developments in the procedures used at the SSCER laboratory for the preparation of Lithium Carbide. *Radiocarbon* **1998**, *40*, 211–214. [[CrossRef](#)]
52. Ramsey, C.B. Bayesian analysis of radiocarbon dates. *Radiocarbon* **2009**, *51*, 337–360. [[CrossRef](#)]
53. Reimer, P.J.; Bard, E.; Bayliss, A.; Beck, J.W.; Blackwell, P.G.; Bronk Ramsey, C.; Grootes, P.M.; Guilderson, T.P.; Haflidason, H.; Hajdas, I.; et al. IntCal13 and Marine13 Radiocarbon Age Calibration Curves 0–50,000 Years cal BP. *Radiocarbon* **2013**, *55*, 1869–1887. [[CrossRef](#)]
54. Svendsen, J.I.; Alexanderson, H.; Astakhov, V.I.; Demidov, I.; Dowdeswell, J.A.; Funder, S.; Gataullin, V.; Henriksen, M.; Hjort, C.; Houmark-Nielsen, M.; et al. Late Quaternary ice sheet history of northern Eurasia. *Quat. Sci. Rev.* **2004**, *23*, 1229–1271. [[CrossRef](#)]
55. Mol, J. Definition of time slices. Landscape and climate change during the Last Glaciation in Europe; A review. In *Evolution of the European Ecosystems during Pleistocene—Holocene transition (24–8 kyr BP)*; Markova, van Kolfschoten, T., Eds.; KMK Scientific Press Ltd.: Moscow, Russia, 2008; pp. 73–91.
56. Kovaleva, N. Northern Tien-Shan paleosol sedimentary sequences as a record of major climatic events in the last 30,000 years. *Revista Mexicana de Ciencias Geológicas* **2004**, *21*, 71–78.
57. Khokhlova, O.S.; Khokhlov, A.A.; Kuznetsova, A.M.; Stolpnikova, E.M.; Kovaleva, N.O.; Lyubin, V.P.; Belyaeva, E.V. Carbonate features in the uppermost layers of Quaternary deposits, Northern Armenia, and their significance for paleoenvironmental reconstruction. *Quat. Int.* **2016**, *418*, 94–104. [[CrossRef](#)]
58. Markova, A.K.; Van Kolfschoten, T.; Bohncke, S.; Kosintsev, P.A.; Mol, J.; Puzachenko, A.Y. *Evolution of the European Ecosystems during Pleistocene—Holocene transition (24–8 kyr BP)*; Scientific Press Ltd.: Moscow, Russia, 2008.
59. Simakova, A.N.; Puzachenko, A.Y. Paleovegetation of Europe during the Bölling-Alleröd interstadial complex warming (12.4–10.9 ka BP). *Polish Geol. Inst. Spec. Pap.* **2005**, *16*, 116–122.



© 2020 by the authors. Licensee MDPI, Basel, Switzerland. This article is an open access article distributed under the terms and conditions of the Creative Commons Attribution (CC BY) license (<http://creativecommons.org/licenses/by/4.0/>).